THE JOURNAL OF COMPARATIVE NEUROLOGY 371:448–460 (1996)

Influence of Mitochondrial Protein Synthesis Inhibition on Deafferentation-Induced Ultrastructural Changes in Nucleus Magnocellularis of Developing Chicks

MAIKE HARTLAGE-RÜBSAMEN AND EDWIN W RUBEL
Virginia Merrill Bloedel Hearing Research Center, Department of Otolaryngology-Head and Neck Surgery, University of Washington, Seattle, Washington 98195

ABSTRACT

Following cochlea removal in developing chicks, about 30% of the neurons in the ipsilateral second-order auditory nucleus, nucleus magnocellularis, undergo cell death. Administration of chloramphenicol, a mitochondrial protein synthesis inhibitor, results in a pronounced increase in deafferentation-induced cell death. In this study, we examined whether the chloramphenicol enhancement of deafferentation-induced cell death reveals the same ultrastructural characteristics that are seen in degenerating nucleus magnocellularis neurons after cochlea removal alone.

Unilateral cochlea removal was performed on anaesthetized posthatch chicks. One group of animals was simultaneously treated with chloramphenicol. Six, twelve, or twenty-four hours following cochlea removal, n. magnocellularis neurons were studied by routine transmission electron microscopy. Particular attention was paid to the integrity of the polyribosomes and rough endoplasmic reticulum.

Two ultrastructurally different types of neuronal degeneration were observed in the deafferented nucleus magnocellularis neurons: an early onset electron-lucent type that always involved ribosomal dissociation and a late-onset electron-dense type displaying nuclear pyknosis and severely damaged mitochondria. The percentage of nucleus magnocellularis neurons displaying ribosomal disintegration following cochlea removal was found to be markedly increased after chloramphenicol treatment. This finding suggests that mitochondrial function is important for the maintenance of a functional protein synthesis apparatus following deafferentation.

Indexing terms: deafferentation, ribosomes, n. magnocellularis, protein synthesis, neuronal death

Studies of neuronal cell death have led to the development of a number of preparations in which to study this process (review: Oppenheim, 1991). Although the course of degeneration may be characteristic for a particular model, some physiological alterations are prevalent in dying cells. Early-onset inhibition of protein synthesis is one of the most widely observed features of degenerating neurons (apoptosis: Clarke, 1990; Houge et al.,1993; deafferentation-induced cell death during development: Pilar and Landmesser, 1976; Steward and Rubel, 1985; Born and Rubel, 1988; developmental cell death: O'Connor and Wyttenbach, 1974; Furber et al., 1987; glutamate toxicity: Vornov and Coyle, 1991; hypoglycemia: Kiessling et al., 1982; ischemia/anoxia: Hossmann and Kleihues, 1973; Lipton, 1987; Widman et al., 1991), and is considered to be one key element in the sequence of cellular changes leading to cell death. However, the inter- and intracellular events that cause this dramatic metabolic breakdown remain a matter of debate.

The cascades of cellular events leading to cell death or survival after a challenge to the environment of a neuron are not well understood. Instead of examining a single metabolic or physiological event, we have stressed that it is helpful to carefully examine the interaction of cellular changes. Deafferentation-induced cell death in the second-order auditory nucleus of the developing chick brainstem,

Accepted April 24, 1996.

Address reprint requests to Edwin W Rubel, Virginia Merrill Bloedel Hearing Research Center, Box 357923, University of Washington, Seattle, WA 98195; E-mail: rubel@u.washington.edu

nucleus magnocellularis (NM), appears to be a suitable model for this purpose. In postnatal chicks (up to 6 weeks of age), removing or electrically silencing the basilar papilla (cochlea) causes transneuronal cell death of about 30% of NM neurons and atrophy of the surviving neurons (Born and Rubel, 1985, 1988). The chronology of early-onset changes seen in degenerating NM neurons have been documented in detail by using a variety of methods including ultrastructure, electrophysiology, histochemistry, immunocytochemistry, autoradiography, and Ca^{2+}-imaging (Durham and Rubel, 1985; Rubel et al., 1990; Garden et al., 1994; Garden et al., 1995a,b; Hyde and Durham, 1990, 1994a; Zirpel et al., 1995). As a result, it has become clear that two seemingly contrary cascades of events dominate intracellular changes in activity-deprived NM neurons. On the one hand, essential anabolic metabolism, such as protein synthesis and RNA synthesis, greatly decreases in the entire population of NM neurons from about 0.5 to 3 hours after afferent activity deprivation (Steward and Rubel 1985; Born and Rubel 1988; Garden et al. 1995a,b). Thereafter, by 6 hours of deprivation, a bimodal distribution of macromolecular synthesis develops; RNA synthesis and protein synthesis return to near normal levels in surviving neurons but cease completely in neurons destined to die (Steward and Rubel, 1985; Born and Rubel, 1988; Garden et al., 1995a,b). The latter state is ultrastructurally reflected by dissolution of cytoplasmic polyribosomes (Rubel et al., 1991). In contrast to the down-regulation of anabolic activity, energy metabolism is up-regulated throughout NM neurons during this period. Activity of several enzymes of the respiratory chain as well as mitochondrial volume increase substantially in NM neurons by 6–12 hours following activity deprivation (Durham and Rubel, 1985; Hyde and Durham, 1990; Durham et al., 1993; Hyde and Durham, 1994a). We have speculated that the up-regulation of mitochondrial function is essential for cell survival. This assertion is supported by the outcome of a study in which chloramphenicol (CAP), an inhibitor of protein synthesis in mitochondria, was used to experimentally prevent the increase in mitochondrial activity of deafferented NM neurons. When chicks are systemically treated with CAP for 12 hours following loss of afferent input, neuronal cell death in NM is markedly increased compared to deprived NM neurons in animals that were not treated with the inhibitor (Hyde and Durham, 1994b; Garden et al., 1994).

In order to interpret the role of mitochondria in cell survival, it is essential to know if the enhanced cell death of NM neurons following chloramphenicol administration is due to enhancement of the deafferentation-induced mechanism itself, or if it is caused by induction of a separate sequence of intracellular events such as increased drug susceptibility of the deprived NM neurons. In the present report, we evaluated dissociation of cytoplasmic polyribosomes as an indicator of deafferentation-induced cell death.

The experimental procedure was to unilaterally remove the cochlea of neonatal chicks, and to allow the animals to survive for 6–24 hours. During the survival period, the experimental animals were systemically treated with CAP; another group of animals received unilateral cochlea removal and vehicle treatment. The percentage of NM neurons displaying complete dissociation of cytoplasmic ribosomes was compared between CAP-treated and vehicle-treated animals. The development of ribosomal dissociation due to inhibition of mitochondrial upregulation was used to discuss a possible basis for the dependence of protein synthesis on mitochondrial activity.

TABLE 1. Overview of Different Treatment Groups

Experimental group	Survival after CR	Treatment	Analysis	Number of animals
V-6	6 h	hourly saline-injection	quantitative	2
CAP-6	6 h	hourly CAP-injection	quantitative	3
V-12*	12 h	12 h saline-pump	quantitative	2
CAP-12*	12 h	12 h CAP-pump	quantitative	6
V-24*	24 h	12 h saline-pump + 12 h survival	qualitative	2
CAP-24*	24 h	12 h CAP-pump + 12 h survival	qualitative	2

*In treatment groups V-12 and CAP-12 osmotic pumps ran for 12 hours after cochlea removal until the animals were sacrificed; in groups V-24 and CAP-24 pumps were removed after 12 hours and animals were allowed to survive for an additional 12 hours.

MATERIALS AND METHODS

Animals and experimental groups

Seventeen 10–14-day-old White Leghorn chickens (H&N International, Redmond, WA) were used as experimental animals. The animals were allowed free access to food and water. All procedures involving the care and treatment of animals were approved by the University of Washington Animal Use Committee.

Survival times following removal of the cochlea (CR) were 6, 12, and 24 hours. In the CAP-treatment group, animals were systemically treated with chloramphenicol during and following CR surgery. In the vehicle-treated group, one cochlea was removed but drug treatment was replaced by saline solution. An overview of treatment groups is given in Table 1.

Surgery

Unilateral cochlea removal was performed as previously described (Born and Rubel, 1985). Briefly, the animal was anesthetized with ketamine hydrochloride (I.M., 80 mg/kg) and Nembutal (I.P., 18 mg/kg), and the right external ear canal was widened with a small incision. The tympanic membrane and columella were removed with small forceps. The basilar papilla (cochlea) was then pulled out through the oval window and was microscopically examined to verify complete removal. The opening was filled with Gelfoam and the skin was sealed with cyano-acrylate glue.

Chloramphenicol administration

Chloramphenicol treatment was modified from protocols previously described in detail (Hyde and Durham 1994b; Garden et al., 1994). Thirty to sixty minutes prior to CR, CAP-treated animals received an initial intramuscular injection 5 mg/100 g body weight of chloramphenicol (chloramphenicol Na-succinate [CAP]; Lyphomed, Deerfield, IL). Subsequently, CAP was administered at a final dosage of 1,000 mg/kg/day by either multiple injections or an implanted Alzet mini-osmotic pump (model 2001D, Alza Corp., Palo Alto, CA). Pumps were filled with CAP that was dissolved in sterile saline (500 mg/ml) and primed by immersion in sterile saline at 37°C for 3 hours. For vehicle-treated animals the CAP-solution was replaced by equal volumes of saline.

Animals that were deafferented and then allowed to survive for 6 hours (treatment groups V-6 and CAP-6) received hourly injections of CAP or vehicle. For 12-hour survival times (groups V-12 and CAP-12), the osmotic

pump was implanted shortly before cochlea removal by briefly anesthetizing the animal, making a small incision in the back, and then placing the pump in the subcutaneous pocket. The incision was closed with cyano-acrylate glue. Animals that survived for 24 hours after CR (groups V-24 and CAP-24) received the same treatment as animals in the 12-hour groups except that 12 hours after CR the osmotic pumps were removed and the animals were allowed to survive for an additional 12 hours.

Tissue processing

Following survival times of 6, 12, or 24 hours, animals were deeply anaesthetized and transcardially perfused. A brief saline washout was followed by 2% paraformaldehyde, 2–2.5% glutaraldehyde in 0.001% $CaCl_2$ in 0.13M Na-cacodylate buffer (pH 7.4). The brains were removed and immersed for 4–18 hours at 4°C in the same fixative. Brains were washed in buffer and 70–100-μm-thick Vibratome sections of the brainstems were cut in the coronal plane. Sections were collected between 30–70% of the rostrocaudal extent of nucleus magnocellularis (NM), processed for routine transmission electron microscopy (TEM), and flat-embedded in Spurr's epoxy resin.

For ultrastructural analyses, one Vibratome section corresponding to 50% of the rostro-to-caudal extent of NM was selected. The regions containing the ipsilateral and contralateral NM were first cut out coarsely with a razor blade. These small blocks were remounted and semithin sections (1 μm) were cut to use as reference for precise trimming of the block to include only the entire region of NM. Ultrathin sections (~80 nm) were then cut on a Reichert Ultracut S, mounted on Formvar-coated slotted grids, stained with uranyl acetate and lead, and viewed on a Philips EM 410 or a JEOL 1200EX transmission electron microscope at 80 kV.

SAMPLING AND CELLULAR ANALYSES

Effect of chloramphenicol on dissociation of ribosomes. Quantitative analysis of the effect of CAP-treatment on ribosomal integrity in deafferented NM neurons was performed for animals in the 6- and 12-hour survival groups. In order to assess whether degenerated neurons were equally distributed in the transverse plane, low-power montages of NM were made for each side of the brainstem. The medial-to-lateral extent of the nucleus was then divided into four compartments (I–IV) of equal width (Fig. 1). For animals killed 6 hours after CR (groups V-6 and CAP-6) all neurons (48 to 88) on the ipsilateral side were photographed. For animals in the 12-hour survival groups (V-12 and CAP-12) ipsilateral NM neurons were assigned consecutive numbers, and 50% of the NM neurons were selected using a random numbering algorithm (with the provision that the sample must include at least 8 neurons in each compartment). This resulted in 32 to 48 neurons for each ipsilateral NM. On the side of the brain contralateral to CR, systematic examination of NM ultrastructure prior to sampling showed no indication of ribosomal disintegration in NM neurons in CAP-treated or vehicle-treated animals. However, 20 neurons from the contralateral NM of each animal were included in the sampling to verify the accuracy of our rating system; five cells from each of the four mediolateral compartments were randomly selected at low power. These sampling methods yielded a total of 658 NM neurons sampled on the side of the brain ipsilateral to the cochlea removal and 260 neurons on the contralateral side of the brain.

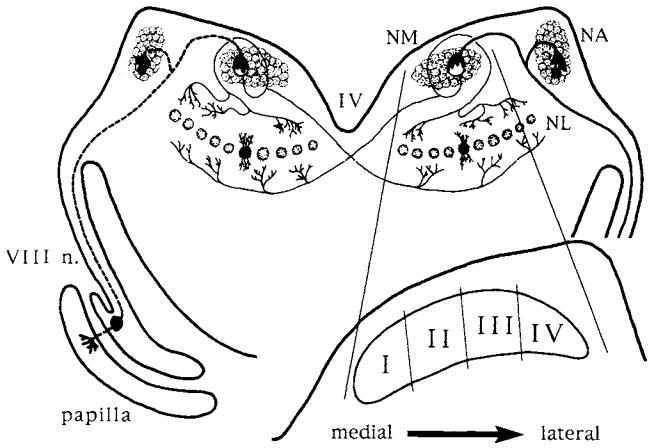

Fig. 1. Schematic diagram of the chick auditory brainstem. NM, nucleus magnocellularis; NA, nucleus angularis; NL, nucleus laminaris; VIIIn, auditory nerve. Inset shows the mediolateral compartmentation of NM used for differential analysis of ribosomal dissociation.

High-power electron micrographs (×10,200) were taken of the cytoplasm of each sampled neuron and enlarged to a final magnification of ×25,092 for the analyses described below. Each sampled neuron was first identified at low power. The magnification was then increased and a high-power photomicrograph was taken of a randomly selected portion of the cytoplasm. These final electron micrographs encompassed approximately one-quarter of the total cytoplasm of each NM neuron.

Micrographs originating from both sides of the brainstem of both vehicle-treated and of CAP-treated animals were coded and randomized. The ultrastructural integrity of cytoplasmic ribosomes in each of the neurons was independently graded by two investigators, blinded to the origin of the micrographs. A 6-point scale was used to grade the cytoplasmic integrity of each NM neuron; rating criteria were adopted from an earlier study (Rubel et al., 1991). An ultrastructural description of the criteria is given in the Results.

Ultrastructural analysis of different types of degeneration. In addition to the analyses of ribosomal integrity, we counted the number of neurons showing signs of lucent or "dark" degeneration in each of our samples. This was done for NM neurons ipsilateral to the CR in both vehicle and CAP-treated animals at 6- and 12-hour survival times. The same set of micrographs used for the ribosomal analysis was used to estimate the percentage of neurons showing different ultrastructural characteristics of degeneration. At 24 hours survival no attempt was made to quantitate the frequency of the degenerative phenotypes.

RESULTS

Ultrastructural morphology of normal NM neurons

The ultrastructure of normal NM neurons has been described in detail elsewhere (Jhaveri and Morest, 1982a,b; Parks, 1981). A representative neuron is shown at low power in Figure 2. The cell body is rather large (ca. 25 μm diameter) and has a spherical (medial and central part of NM in the transverse plane) to ovoid (lateral part of NM) shape. Cell nuclei are round and usually lie in the center of

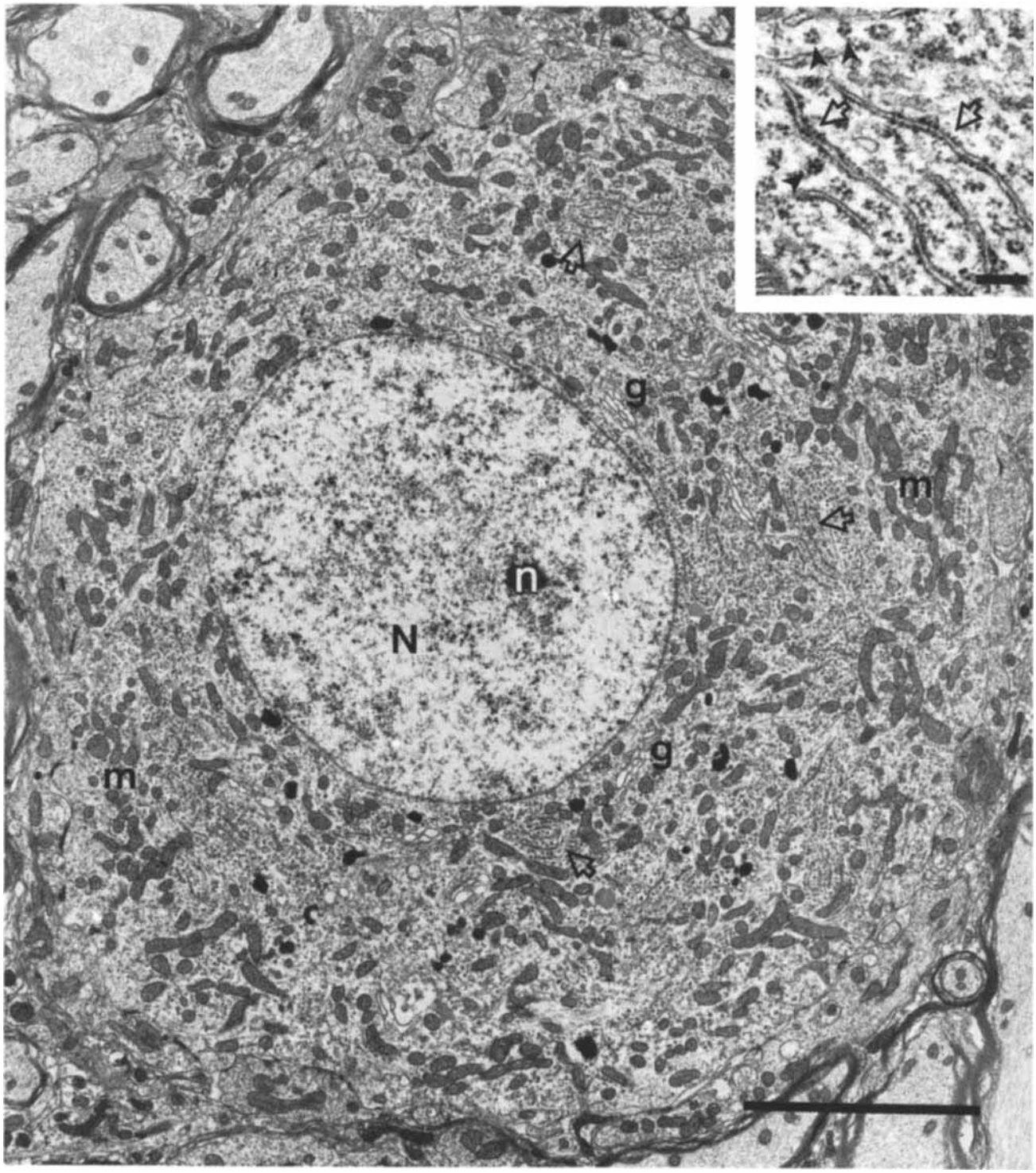

Fig. 2. Transmission electron micrograph of a nucleus magnocellularis (NM) neuron from the normally afferented, control side of the chick brainstem. Nucleus, N; nucleolus, n; mitochondria, m; Golgi complex, g; rough endoplasmic reticulum (open arrows). Bar = 5 μm. **Inset:** Higher magnification of NM neuron cytoplasm showing intact polyribosomes (arrowheads) and rough endoplasmic reticulum with associated ribosomes (open arrows). Bar = 0.2 μm.

the perikaryon. The cytoplasm contains a large number of mitochondria that are distributed throughout the perikarya. The abundance of cytoplasmic ribosomes in the neuronal soma indicates a high level of protein synthesis activity. Ribosomes are either arranged in rosettes as polysomes or they are bound as individual ribosomes to membranes of the endoplasmic reticulum (ER), forming the rough endoplasmic reticulum (RER). RER often forms

stacks of cisternae (Nissl bodies). Golgi complexes, lysosomes, and a few cisternae of smooth ER are observed in the cytoplasm.

Electron-lucent of type degeneration and criteria for rating system

An electron-lucent phenotype of degeneration with dissociated cytoplasmic ribosomes has been described for early time points (3–6 hours) after cochlea removal or activity blockade of the 8th nerve (Rubel et al., 1991). This phenotype was the predominant one seen in both treatment conditions and at all time points studied. It was seen only on the side of the brain ipsilateral to CR, and it was the only degenerative phenotype seen at 6 or 12 hours in vehicle-treated animals. The earliest and most striking feature of affected cells is the loss of functional protein synthesis organelles in the cytoplasm; ribosomes dissociate from RER membranes and polysomes, and ultimately form distinct patches of degraded ribosomal material in the cytoplasm, often near stacks of "denuded" ER membranes (Fig. 3A,B). By 6 hours after CR the entire cytoplasm of a subpopulation of some affected NM neurons was devoid of associated ribosomes, whereas some other neurons were in an intermediate state of ribosomal degradation. A second characteristic of deafferented neurons in groups V-6 and V-12 was the appearance of mitochondria, which increased in length and often formed branches. They were usually concentrated toward the center of the cell, eventually leading to a mitochondria-free margin in the periphery of the cytoplasm. Some neurons also showed intense swelling of the Golgi apparatus, whereas morphology of the ER cisternae remained unaltered.

Other changes in ultrastructure seen at 6 and 12 hours post-CR involved the cell nucleus; it was often displaced toward the periphery of the cell and changed shape from spherical to ovoid. The nuclear membrane was often convoluted and the karyoplasm appeared increasingly granular. In a few cases, breakdown of nuclear membrane was observed (Fig. 3C).

The above ultrastructural profile was true for the great majority of degenerating neurons in the ipsilateral NM of both vehicle-treated (groups V-6 and V-12) and CAP-treated animals (groups CAP-6 and CAP-12). However, vehicle and CAP-treated groups differed in one respect. Whereas mitochondrial volume appeared moderately increased in groups V-6 and V-12, some of the degenerating NM neurons in groups CAP-6 and CAP-12 displayed a huge abundance of mitochondria to the point where the whole cytoplasm was filled with these organelles (see below).

In order to quantify the degree of ribosomal dissociation in NM neurons from CAP-treated vs. vehicle-treated animals, a 6-point scale was established. Typical examples of the cytoplasmic appearance of NM neurons receiving different ratings are shown in Figure 4. The morphological criteria for the rating were as follows: 6) An abundance of ribosomes, both bound to the RER and arranged as polysomes, is present in the cytoplasm. 5) The quantity of ribosomes and polysomes is less abundant, but in both 5 and 6 no dissolution of ribosomal complexes is seen (Fig. 4A). 4) The number of polysomes and RER-bound ribosomes is decreased, and there is some indication of beginning dissolution of ribosomes in some areas of the cytoplasm. 3) Ribosomal dissociation of whole areas in the cytoplasm is more pronounced and beginning formation of ribosomal debris is seen; however, there are still a significant number of polysomes and RER-bound ribosomes present. An example of this intermediate state of ribosomal dissociation is shown in Figure 4B. 2) Polysomes have nearly completely disappeared and RER membranes are almost devoid of ribosomes; there are distinct patches of ribosomal debris. 1) There is no sign of polysomes, RER membranes are denuded, and large patches of ribosomal debris have formed. This final stage of ribosomal dissociation is demonstrated in Figure 4C.

Effect of CAP treatment on ribosomal dissociation

At both 6 and 12 hours after unilateral cochlea removal CAP treatment significantly increased the number of neurons displaying dissociation of the ribosomes from the RER and dissolution of polysomes. These differences are summarized in Figure 5. At 6 hours after CR an average of 44.5% (range = 21–80%; 3 animals; 112 of 243 neurons) of neurons in the ipsilateral NM of CAP-treated animals (CAP-6) were rated 1–2 (complete dissociation of ribosomes) compared to only 10.0% (range = 9–10.5%; 2 animals; 12 of 122 neurons) in group V-6 (Fig. 5A). By 12 hours the proportion of neurons with complete loss of cytoplasmic ribosomes had increased in both groups. In the CAP-treated group (CAP-12) 54.9% (range = 18–74%; 6 animals; 122 of 225 neurons) and in the vehicle-treated group (V-12) 21.5% (range = 13–30%; 2 animals; 15 of 68 neurons) were rated 1–2 (Fig. 5B). During the same time period the percentage of NM-neurons displaying an intermediate state of ribosomal dissociation (3–4) decreased from an average of 11.9% to 5.5% in the CAP-treated groups, and from 11.7% to 4.4% in the vehicle-treated groups, respectively. Statistical analyses using ANOVA (Statview® 5.1) revealed significantly more neurons rated in the 1–2 category in CAP-treated animals than vehicle-treated animals at both time points (P's $< .01$).

Analysis of the rating of NM neurons on the side of the brain contralateral to CR of each animal revealed no effect of CAP treatment alone on ribosomal integrity of the nondeafferented NM neurons. Across all animals, 99.6% of contralateral neurons (n = 260) received a rating of 5–6 (morphologically intact ribosomes); one neuron was rated 3–4.

A more detailed picture of the pattern of deafferentation-induced changes in NM neurons can be obtained by analyzing the distribution pattern of neurons with dissociated ribosomes in the ipsilateral NM. Separate evaluation of the dissociation rate in compartments I–IV suggests a non-uniform distribution of neuronal sensitivity to deafferentation (Fig. 6). In vehicle-treated animals, the variation between compartments was high and the number of animals of each time point too low to provide a clear picture. However, in the CAP-treated animals at both survival times there was a clear trend for neurons in the most medial compartment (Comp. I) to show a higher resistance to the effects of deafferentation than neurons located more laterally (Comp. II–IV). ANOVA revealed that this difference was statistically significant ($P < .05$) at twelve hours (CAP-12), with 31.2% (±12.9% SEM) of neurons affected by ribosomal dissociation in Comp. I compared to 63.2% (±9.0%) and 72.0% (±11.1%) in Comp. II and III, respectively.

Among the six animals in the 12-hour survival CAP-treated group (CAP-12), the percentage of neurons with complete ribosomal dissociation was remarkably lower in one animal than in the other five animals (18.0% [n = 40] in

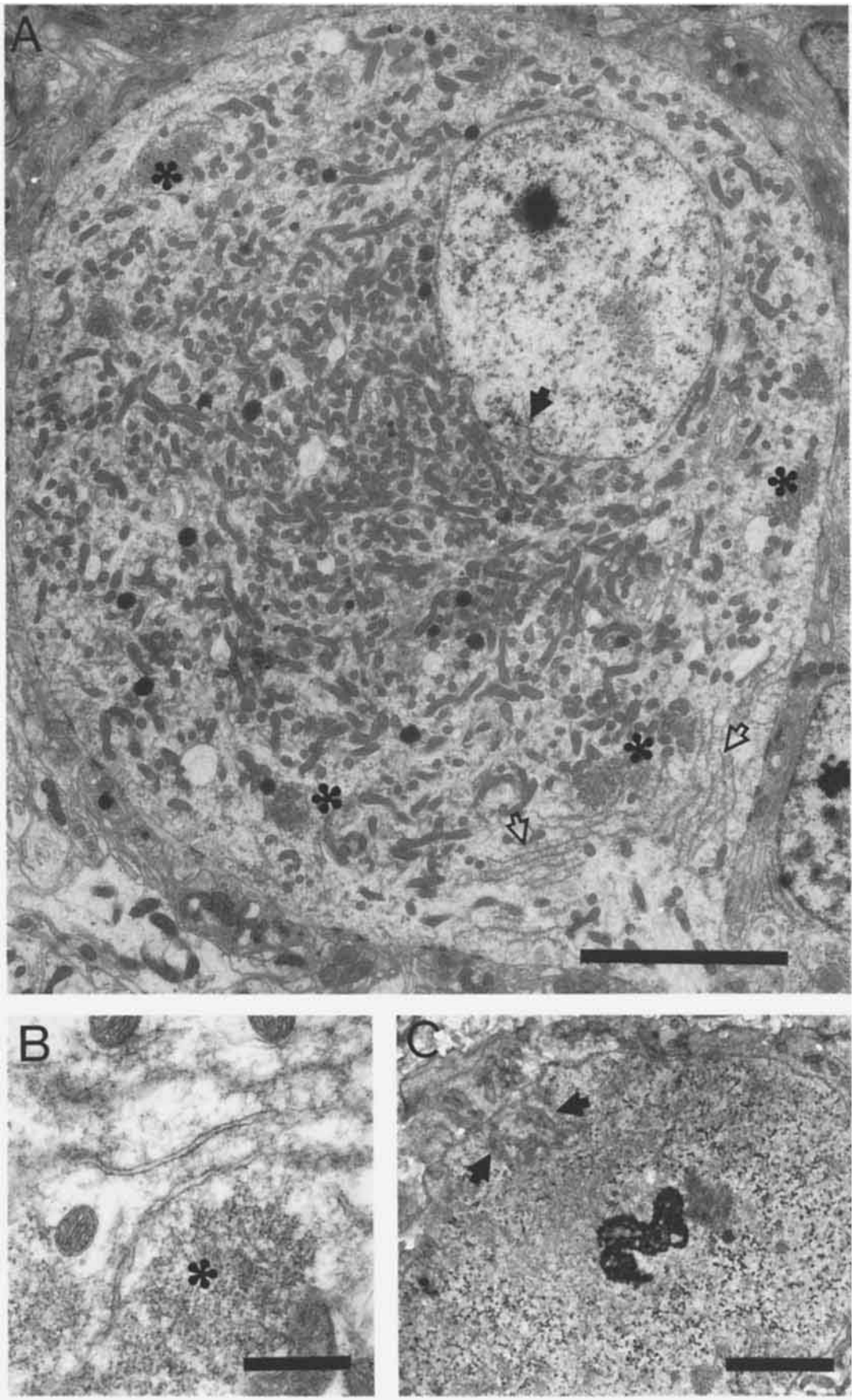

Fig. 3. Electron-lucent type of degeneration 12 hours following cochlea removal. **A:** Transmission electron micrograph of a deafferented NM neuron from a chloramphenicol (CAP)-treated animal displaying complete dissociation of cytoplasmic ribosomes. Note patches of ribosomal debris (asterisks), stacks of rough endoplasmic reticulum devoid of ribosomes (open arrows), and beginning convolution of the nuclear membrane (solid arrows). Bar represents 5 μm. **B:** Detail of the same neuron showing ribosomal dissociation (asterisk). Bar = 0.5 μm. **C:** Breakdown of nuclear membrane in a deafferented NM neuron from a vehicle-treated animal (solid arrows). Bar = 2 μm.

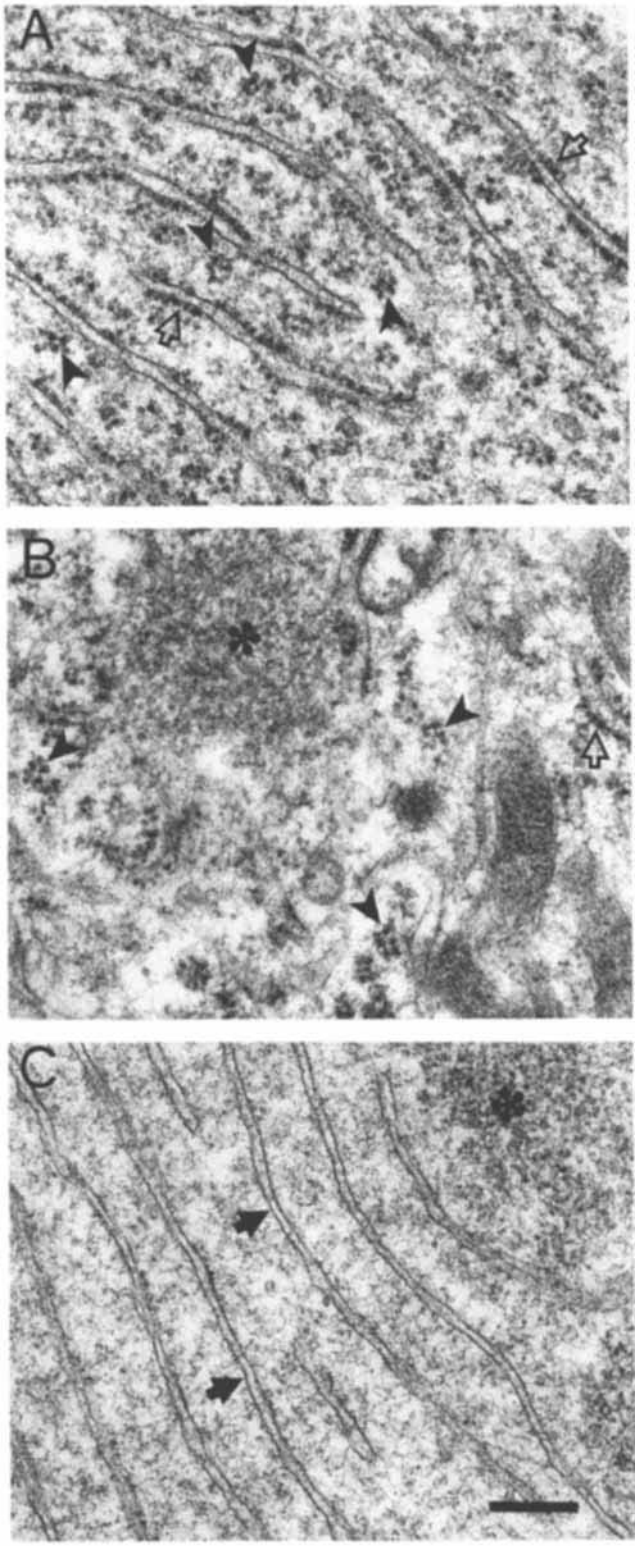

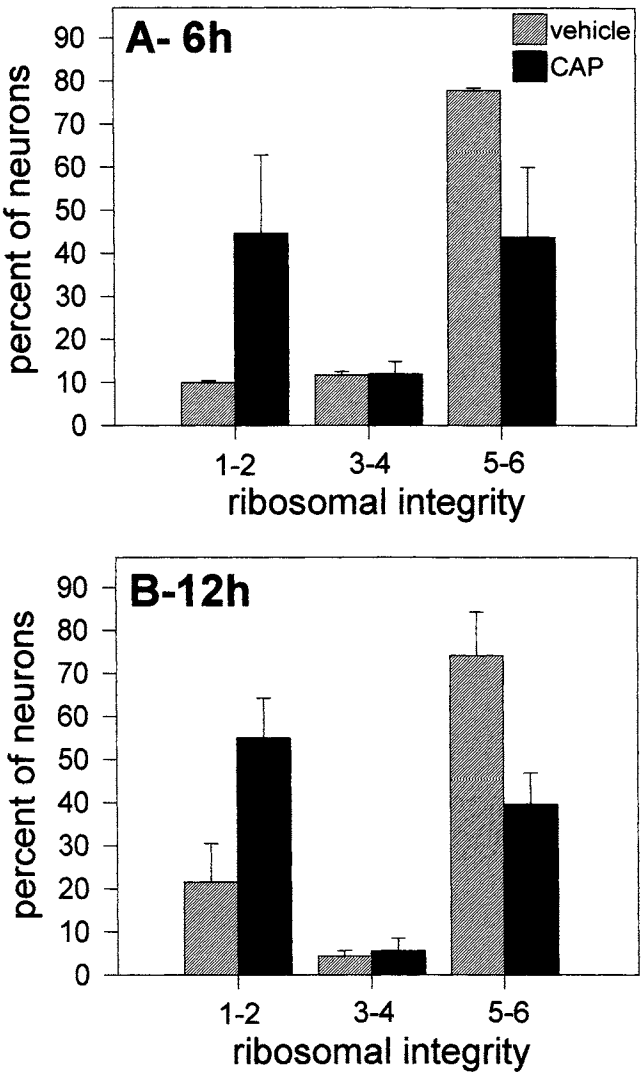

Fig. 5. Ribosomal integrity ratings in deafferented NM neurons from CAP-treated and vehicle-treated chicks sacrificed **A)** 6 hours and **B)** 12 hours after cochlea removal. The abscissa shows different states of ribosomal integrity: 1–2) dissociated ribosomes, 3–4) ribosomes partially dissociated, 5–6) normal-appearing ribosomes. Mean values (±SEM) from CAP-treated animals (solid bars) are compared with those from vehicle-treated animals (hatched bars). Note that groups V-6 and V-12 each had only two animals. Thus SEM is a conservative estimate of the average deviation.

Fig. 4. Examples of ribosomal integrity in NM neurons rated on a 6-point scale. **A:** Cytoplasmic ribosomes are mainly associated (ratings 5 and 6): an abundance of polyribosomes (arrowheads), and ribosomes bound to the rough endoplasmic reticulum (RER; open arrows) are present. No ribosomal debris can be detected. **B:** Intermediate state of ribosomal integrity (ratings 3 and 4): polyribosomes (arrowheads) and/or RER-bound ribosomes (open arrows) are still seen, but there is also formation of patches of ribosomal debris (asterisk). **C:** Cytoplasmic ribosomes appear dissociated (ratings 1 and 2): no polyribosomes are present, RER membranes are devoid of ribosomes (solid arrows), and patches of ribosomal debris have formed (asterisk). Bar = 0.2 μm in A–C.

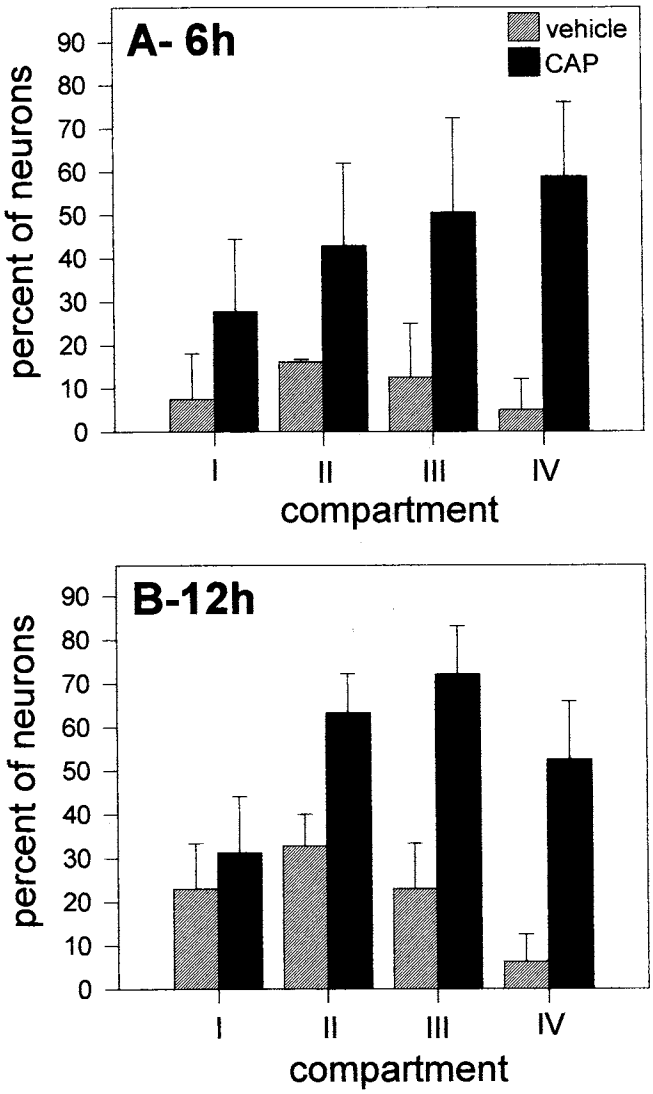

Fig. 6. Distribution of neurons displaying complete ribosomal dissociation along the mediolateral axis of NM **A)** 6 hours and **B)** 12 hours following cochlea removal. The abscissa indicates different compartments (I–IV) along the mediolateral extent of the nucleus. Mean values (±SEM) from CAP-treated animals (solid bars) are compared with those from vehicle-treated animals (hatched bars).

this deviant animal, compared to an averaged 62.9% ± 5.9% SEM [n = 225] in the other five animals). However, in this same animal the number of NM neurons displaying the electron-dense phenotype predominated (32.5%); in other animals of the CAP-12 group very few neurons showed this type of degeneration (see below).

Electron-dense type degeneration

The occurrence of NM neurons displaying an electron-dense type of degeneration was also restricted to neurons on the deafferented side of the brainstem. In the CAP-treated groups of animals this degenerative phenotype was first observed in a very small number of neurons at 6 hours following CR (CAP-6), and in vehicle-treated animals it was only observed at 24 hours post-CR (V-24). Affected neurons could be easily identified due to shrinkage of the cell body, associated with convolution of the cell membrane and a very pronounced increase in electron-density of the cytoplasm (Fig. 7). In addition, the cell nuclei were often elongated, were displaced to the periphery of the cell, and appeared pyknotic. At early stages of degeneration clumping of chromatin occurred (Fig. 7A), whereas at later stages (i.e., 24 hours post-CR) the nucleus was deformed and the karyoplasm became homogeneously electron-opaque (Fig. 7B). Mitochondria were markedly increased in number and appeared extensively swollen with progressive disintegration of the inner cristae. In cells displaying this degenerative phenotype polysomes and ER-membrane-bound ribosomes were only identifiable until 12 hours following cochlea removal (Fig. 7C). By 24 hours mitochondrial proliferation and swelling was so exaggerated that hardly any other cytoplasmic components could be identified (Fig. 7D).

The overall percentage of neurons displaying this electron-dense phenotype in the CAP-treated animals was relatively low at both 6 hours (1.6%) and 12 hours (7.9%), yet the variability between animals was high. In most animals of the CAP-treated groups electron-dense degeneration was observed in neurons that also displayed the characteristic feature of electron-lucent degeneration, dissociation of cytoplasmic ribosomes. However, the electron-dense phenotype was not always paralleled by ribosomal disintegration. In one of the six animals of the CAP-12 group there was a large number of neurons (32%) that showed condensed cytoplasm, swelling of mitochondria, and cell shrinkage, but morphologically intact polysomes. In this animal the percentage of neurons displaying ribosomal dissociation was extremely low (15.0%) compared to neurons from the other five chicks of this treatment group (average: 62.9%; range 69%–44%).

Observations of NM neurons from two vehicle-treated animals 24 hours following CR (group V-24) revealed that electron-dense degeneration also developed in a small number of neurons from the deprived side of the brain. No attempt was made to quantify the degenerative characteristics of neurons in this group. The degree of cellular disintegration in these neurons appeared comparable to neurons from animals which received CAP-treatment for the first twelve hours following CR and then survived for additional twelve hours (group CAP-24). Unfortunately, the morphological integrity of ribosomal complexes in neurons at this survival time could not be assessed due to proliferation and extreme swelling of mitochondria (Fig. 7D).

DISCUSSION

In the present report, we show that inhibition of mitochondrial protein synthesis with chloramphenicol (CAP) after cochlea removal is followed by a marked increase in the number of nucleus magnocellularis (NM) neurons displaying ribosomal disintegration, a marker for afferent deprivation-induced cell death in the developing chick auditory system. In addition, we described a small number of dying neurons that displayed an electron-dense degenerative phenotype.

As in all studies using metabolic inhibitors, interpretation of our results depends on acceptance that the agent we used is causing the desired specific effect, rather than potentiating neuronal degeneration by a general systemic side-effect. Therefore, a discussion of the above results will be preceded by methodological considerations on the use of chloramphenicol.

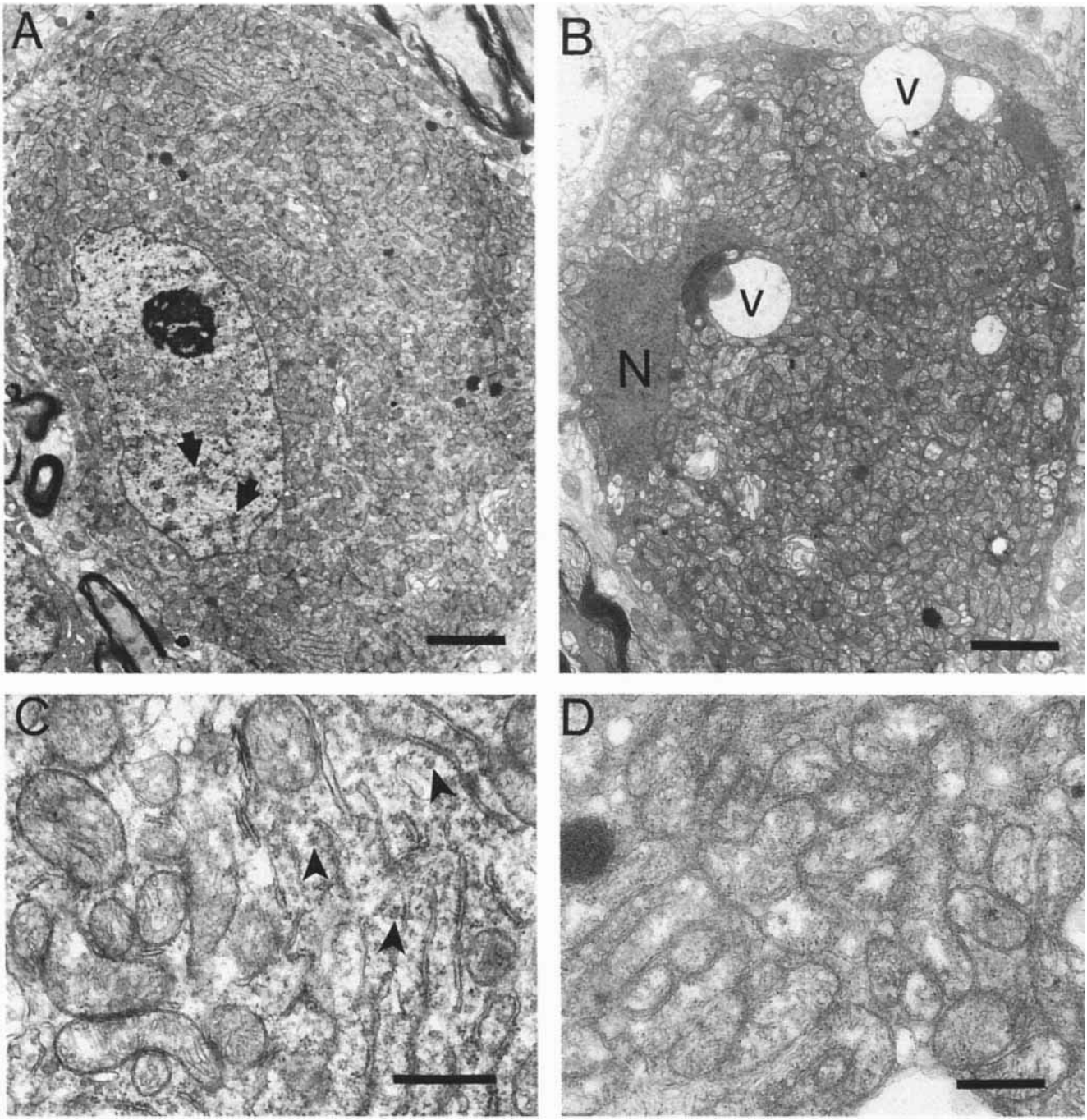

Fig. 7. Electron-dense type of degeneration. **A:** Transmission electron micrograph of a deafferented NM neuron from a CAP-treated animal killed 12 hours following cochlea removal. Note cell shrinkage and initial signs of chromatin clumping (arrows) in the nucleus, which is still electron-lucent. Bar = 2 μm. **B:** Deafferented NM neuron from a CAP-treated animal killed 24 hours following cochlea removal. Note pyknosis and deformation of the nucleus (N) and vacuolization of the cytoplasm (v). Bar = 2 μm. **C:** Detail of the neuron shown in A; some ribosomes are still associated (arrowheads) and mitochondria exhibit some swelling. Bar = 0.5 μm. **D:** Detail of a neuron from the same treatment group as shown in B, demonstrating extreme swelling of the mitochondria and displacement of the cytoplasm. Bar represents 0.5 μm.

Methodology

Chloramphenicol has been widely used clinically as a broad-spectrum antibiotic. It selectively binds to 70S-ribosomes of prokaryotes and mitochondria of eukaryotes, where it blocks protein synthesis through inhibition of the peptidyl transferase action (Jiménez, 1976). The fact that in eukaryotes CAP application leaves cytoplasmic protein synthesis unimpaired (Lamb et al., 1968; Tzagoloff, 1982) makes it a suitable tool for physiological studies on the effects of mitochondrial protein synthesis inhibition.

However, during clinical use in humans, serious toxic side effects have been documented (review: Holt et al., 1993). Besides complications such as bone marrow suppres-

sion and aplastic anemia due to treatment with high CAP doses over several days, effects in human infants and in animals have included severe hypotension and circulatory collapse. Several lines of evidence indicate that one key element in the development of CAP-induced pathogenesis is the generation of hydroxyl and oxygen-free radicals. In neonatal rats these oxidizing agents cause short-term depletion of cellular ATP-stores (Hallmann, 1973), and in vitro studies have shown that they mediate DNA degradation (Murray et al., 1982), lipid peroxidation and oxidation of proteins and carbohydrates (Tocher et al., 1988). Additionally, long-term treatment with CAP may induce mitochondrial damage through protein synthesis inhibition or have effects on electron transport (Yunis, 1988).

In the present study, application of a relatively high dose of CAP (1000 mg/kg/day) was spread over the entire treatment period (not exceeding 12 hours) by either hourly injections or implantation of an osmotic pump. Compared to the animals that were not treated with the mitochondrial inhibitor, the chicks receiving this drug were similar in their activity levels and behavior. The only observed side effect was that CAP-treated animals usually took longer to wake from the anesthesia, suggesting a mild hypotensive effect of the treatment. Thus, we believe that systemic short term CAP-treatment did not lead to serious impairment of the animals' general condition that might have distorted the experimental outcome. In addition, no deleterious effects of CAP could be detected in the ultrastructure of NM neurons contralateral to cochlea removal. However, possible interference of either chloramphenicol itself or of its metabolites with *specific* intracellular processes other than mitochondrial protein synthesis (that are induced by afferent deprivation) cannot be ruled out completely and will be discussed briefly below.

In some neurons of the ipsilateral NM of CAP-treated animals we observed a very high increase in the number of mitochondria following cochlea removal. This apparent inconsistency can be explained on the basis of genetic studies of mitochondrial biogenesis in lower eukaryotes. "Petite" yeast mutants that lack mitochondrial DNA cannot synthesize proteins in their mitochondria. Nevertheless, they contain (nonrespiring) mitochondria (Montisano and James, 1979) whose biogenesis is regulated by the cell nucleus (Tzagoloff and Myers, 1986; Attardi and Schatz, 1988). Thus, it is reasonable to assume that newly proliferated mitochondria, which are found in NM neurons in spite of mitochondrial protein synthesis inhibition, lack key building blocks required for normal function.

Effect of CAP on ribosomal integrity

The present study is based on previous reports demonstrating that after deprivation of afferent input mitochondrial volume, cytochrome c oxidase activity and succinate dehydrogenase activity are upregulated in NM neurons (Durham and Rubel, 1985; Hyde and Durham, 1990; Hyde and Durham, 1994a), and that blockade of this mitochondrial upregulation with CAP results in increased cell death (Hyde and Durham, 1994b). In the present report we show that removal of the cochlea in combination with CAP-treatment leads to a dramatic increase in the number of ipsilateral NM neurons which display ribosomal dissociation compared to deafferented NM neurons in unmedicated animals. This finding is consistent with the results of a recent investigation from our laboratory examining the influence of CAP on immunolabeling patterns of NM neurons by a monoclonal antibody against ribosomal RNA (*y10b:* Steitz, 1989). CAP application increases the number of NM neurons that fail to recover *y10b* immunoreactivity following CR (Garden et al., 1994).

Since dissociation of cytoplasmic ribosomes appears to be an early marker for NM neurons which are destined to die in response to afferent deprivation (Rubel et al., 1991), it appears that the increased cell death due to inhibition of mitochondrial up-regulation involves the same degenerative mechanism(s) that cause neurons to die after deafferentation alone. In other words, up-regulated mitochondrial function is likely to promote survival of NM neurons by directly or indirectly affecting one or several steps in the cascade of events that lead to cell death.

In intact cells the main role of mitochondria is to coordinate key reactions in cell energy metabolism, i.e., citric acid cycle and oxidation of fatty acids (Alberts et al., 1989). Additionally, the inner mitochondrial membrane contains a Ca^{2+}-specific uniporter that enables mitochondria to take up Ca^{2+} into the matrix (Lehninger, 1970). Considering the energy-converting function of mitochondria, it appears paradoxical that while all ATP-requiring cellular activity studied so far in activity-deprived NM neurons is either abolished (electrical activity: Born et al., 1991) or down-regulated (protein synthesis: Born and Rubel, 1988; RNA-synthesis: Garden et al., 1995a), mitochondrial function in the deafferented NM is upregulated. The most likely explanation for upregulation of the energy metabolism of NM neurons in response to deafferentation involves a change in the intracellular Ca^{2+} concentration ($[Ca^{2+}]_i$), that has been shown to be a common feature of degenerating neurons. There is considerable evidence for a close interaction between intracellular Ca^{2+} content and mitochondrial metabolism (Fein and Tsacopoulos, 1988; Denton and McCormack, 1990; Werth and Thayer, 1994; Herrington et al., 1996). In addition, when challenged with high $[Ca^{2+}]_i$, mitochondria are capable of sequestering large Ca^{2+} loads (Prentki et al., 1984) by using the energy provided by the electrical gradient across the inner mitochondrial membrane (Denton and McCormack, 1990; Herrington et al., 1996). Ultimately, sustained elevation of intracellular Ca^{2+} leads to depletion of cellular energy supply, which is a widely described effect of Ca^{2+}-mediated toxicity (Cheung et al., 1986; Siesjö, 1988). Both uncoupling of oxidative phosphorylation and Ca^{2+} pump activities decrease the intracellular ATP:ADP ratio which regulates mitochondrial function (Brand and Murphy, 1987) and are thus reasonable candidates to cause mitochondrial up-regulation following deafferentation in NM neurons.

In vivo and in vitro studies on NM neurons have shown an increase in cytoplasmic $[Ca^{2+}]$ in unstimulated neurons as early as 1–2 hours following CR (Zirpel et al., 1995; Zirpel and Rubel, 1996). This is consistent with a growing literature showing that increases or decreases in $[Ca^{2+}]$ are key events in the sequence of events leading to cell death in a variety of systems (Choi, 1987; Choi, 1988a; Randall and Thayer, 1992; Simon et al., 1984; Siesjö, 1988; Choi, 1988b; Boobis et al., 1989; Orrenius et al., 1989; McConkey et al., 1989; Trump and Berezesky, 1992; Orrenius et al., 1992).

In summary, it appears reasonable to hypothesize that upregulated respiratory chain activity, seen in both surviving and degenerating NM neurons in response to afferent activity deprivation (Hyde and Durham, 1990; 1994a), is likely to be a consequence of a sustained increase in $[Ca^{2+}]_i$.

CAP treatment prevents this response, resulting in greater neuronal death. We would further hypothesize that this potentiation of neuronal death is a consequence of the fact that preventing mitochondrial upregulation increases the number of neurons that fail to reestablish cytoplasmic ionic and/or energy homeostasis after loss of afferent input.

Influence of mitochondrial function on protein synthesis and cell death

Early-onset inhibition of macromolecular synthesis is a common feature of cell death in a variety of neural and non-neural systems. For example, protein synthesis inhibition is seen in neurons following ischemia (Hossmann and Kleihues, 1973; Raley-Susman and Lipton, 1990; Krause and Tiffany, 1993), anoxia in hippocampal slices (Lipton et al., 1988), hypoglycemia (Agardh et al., 1978; Bergstedt et al. 1993), and glutamate neurotoxicity (Vornov and Coyle, 1991). In all of these reports changes in ion homeostasis or ATP-depletion of the challenged neurons are predictive of the onset of protein synthesis inhibition. Debate about the relative importance of ionic composition and ATP is probably moot since translational activity is equally dependent on energy supply (Jagus et al., 1981; Kleihues and Hossmann, 1971) and ionic composition of the cytoplasm (Jones and McIlwain, 1971; Moore and Spremulli, 1985), and since these factors are intimately related (e.g. Mattson et al., 1993). The cascade of cellular events leading to cell death and cell survival in NM is likely to involve similar conditions. As noted above, a significant increase in $[Ca^{2+}]_i$ occurs rapidly in NM neurons after afferent deprivation. Intracellular Ca^{2+} and energy production are controlled by mitochondrial activity. As such, they are the most likely candidates to explain the linkage between mitochondrial and ribosomal function in NM neurons.

Although we believe that changes in $[Ca^{2+}]_i$ represent pivotal events that mediate between mitochondrial and ribosomal function in NM neurons, a detailed examination of the temporal patterns of protein synthesis activity, ribosomal function and ribosomal structure following afferent deprivation yields a complex picture. There appear to be at least three phases. i) Initial phase (0.5–3 hours post-CR): protein synthesis and RNA synthesis are dramatically decreased in all NM neurons, but ribosomes are still assembled to polysomes and line RER membranes. ii) Reversible phase (3–6 hours post-CR): complete cessation of protein synthesis activity occurs in a portion of NM neurons and is paralleled by the disassembly of ribosomes in the same neurons, but restoration of afferent activity will prevent cell death and normal ultrastructure will be regained (Born and Rubel, 1988; Rubel et al., 1991). iii) Final phase (6–24 hours post-CR): irreversible cessation of protein synthesis in a portion of neurons is accompanied by complete dissociation and degradation of cytoplasmic ribosomes, which is reflected by increased density of ribosomal debris and culminates in cell death.

The ultrastructure of ribosomes in a cell undergoing suppression of protein synthesis may be indicative of which step of the translational process is inhibited (Jagus et al., 1981). During the initial phase of protein synthesis inhibition, the presence of polysomes and RER-bound ribosomes indicates that polypeptide chain elongation is depressed. During the second and final phases polypeptide chain initiation is blocked, which is reflected by dissociation of ribosomes (Kleihues and Hossmann, 1971; Krause and Tiffany, 1993). It is intriguing to compare this sequence of

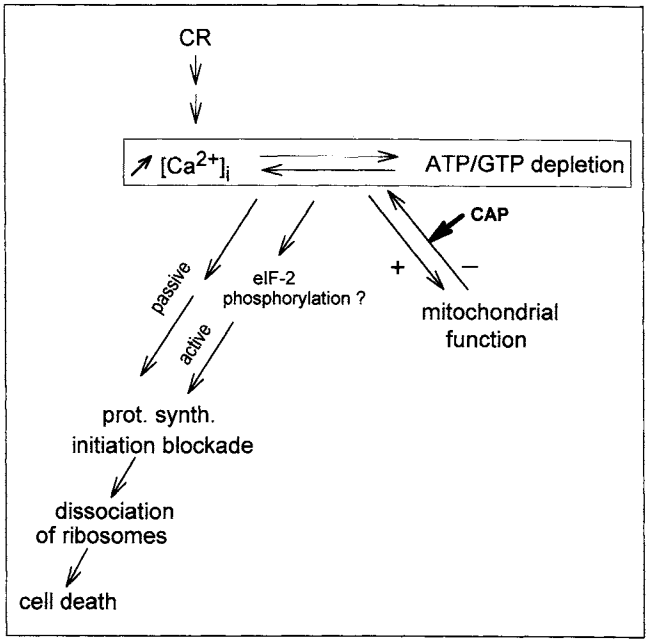

Fig. 8. Model of the hypothesized relationship between mitochondrial and ribosomal function in NM neurons in response to deafferentation. +, increase; −, decrease (see Discussion).

changes and the changes we have described in NM neurons to investigations of protein synthesis suppression in two other well-studied systems of neuronal injury, cerebral ischemia (Kleihues and Hossmann, 1971; reviewed by: Krause and Tiffany, 1993) and neocortical hypoglycemia (Bergstedt et al., 1993). In these systems inhibition of the elongation step is paralleled by ATP/GTP depletion and maintenance of the ultrastructural polysome profile. During early reperfusion or recovery from hypoglycemia, suppression of the initiation step is ultrastructurally mirrored by complete dissolution of polysomes. Further disintegration of the intracellular environment is believed to be responsible for irreversible breakdown of protein synthesis.

In both of the above models of neuronal cell death active regulation involving eukaryotic initiation factor-2 (eIF-2) has been suggested to cause blockade of protein synthesis initiation during the second stage. The eIF-2 protein regulates a well studied, rate-limiting step in cellular protein synthesis initiation (Merrick, 1990; Morley and Thomas, 1991; Sarre, 1989). In its active form eIF-2 allows assembly of ribosomal subunits in order to form a functional ribosome (Rhoads, 1993), whereas only partially phosphorylated eIF-2 causes complete, but reversible, suppression of polypeptide chain initiation (Hershey, 1990). During recovery from hypoglycemia eIF-2 activity was demonstrated to be decreased by 42% (Bergstedt et al., 1993). Furthermore, activity of eIF-2 has been found to be blocked in a variety of cells under diverse forms of stress (Panniers and Henshaw, 1983). It will be of interest to determine whether eIF-2 also plays a role in the change we have observed in NM neurons.

In summary, an excess of intracellular Ca^{2+} is hypothesized to play a key role in mediating the effects of activity deprivation on NM neurons. If this is the case, the model shown in Figure 8 appears to best match our current knowledge. Deafferentation-induced disruption of intracellular ion and energy homeostasis causes both upregulation

of mitochondrial function and down-regulation of protein synthesis. Upregulation of mitochondrial function may contribute to diminishing the effects of deafferentation through increased energy production and/or Ca^{2+} sequestration. Consequently, blockade of mitochondrial upregulation results in an increase in the number of NM neurons displaying ribosomal dissociation following CR. There is no evidence that breakdown of ribosomes itself triggers upregulation of mitochondrial function.

Electron-dense type of degeneration

In addition to the electron-lucent type of degeneration seen in the majority of dying NM neurons, we found neurons displaying a different degenerative phenotype in the NM neurons deprived of afferent input. The main characteristics of these neurons are shrunken cell bodies, nuclear pyknosis, eosinophilic cytoplasm, and extremely swollen mitochondria with disrupted inner mitochondrial membranes. At 12 hours post-CR this electron-dense degeneration was restricted to a small number of neurons in three out of six CAP-treated animals, with neurons from one chick demonstrating particular sensitivity to this kind of degenerative alteration. In this animal, electron-dense degeneration was found in a number of neurons that did not show signs of ribosomal dissociation. Thus, it must be noted that in animals receiving CAP the electron-dense degenerative phenotype can develop independently from the electron-lucent phenotype.

Extreme swelling of mitochondria can be due to loss of inner membrane integrity because of excessive mitochondrial uptake and release of Ca^{2+} ("Ca^{2+}-cycling"; Orrenius et al., 1992; Mattson et al., 1993), in combination with Ca^{2+}-induced generation of prooxidants/free radicals (Choi, 1988a; Richter and Kass, 1991). Oxidative mitochondrial damage caused by excess intracellular calcium would be a secondary effect of CR, possibly explaining the delayed appearance of this degenerative phenotype. In this respect, it will be interesting to assess the role of bcl-2, a protein often localized to the inner mitochondrial membrane, since bcl-2 is known to prevent apoptosis in some injured cells by scavenging free radicals (Hockenbery et al., 1993; Kane et al., 1993).

ACKNOWLEDGMENTS

The authors thank Dale Cunningham for expert technical assistance, Gwenn Garden and Diana Lurie for help in the rating of a never-ending number of electron micrographs, Lance Zirpel for comments on an earlier version of the manuscript, and Heinz Schwarz for manifold support. This work was supported by NIH grant DC 00520.

LITERATURE CITED

Agardh, C.D., J. Folbergrová, and B. Siesjö (1978) Cerebral metabolic changes in profound, insulin-induced hypoglycemia, and in the recovery period following glucose administration. J. Neurochem. *31:*1135–1142.

Alberts, B., D. Bray, J. Lewis, M. Raff, K. Roberts, and J.D. Watson (1989) Molecular biology of the cell. New York: Garland Publishing, pp. 342–366.

Attardi, G. and G. Schatz (1988) Biogenesis of mitochondria. Ann. Rev. Cell Biol. *4:*289–333.

Bergstedt, K., B.R. Hu, and T. Wieloch (1993) Initiation of protein synthesis and heat-shock protein-72 expression in the rat brain following severe insulin-induced hypoglycemia. Acta Neuropathol. *86:*145–153.

Boobis, A.R., D.J. Fawthrop, and D.S. Davies (1989) Mechanisms of cell death. TiPS *10:*275–280.

Born, D.E. and E.W Rubel (1985) Afferent influences on brainstem auditory nuclei of the chicken: Neuron number and size following cochlea removal. J. Comp. Neurol. *231:*435–445.

Born, D.E. and E.W Rubel (1988) Afferent influences on brainstem auditory nuclei of the chicken: Presynaptic action potentials regulate protein synthesis in nucleus magnocellularis. J. Neurosci. *8:*901–919.

Born, D.E., D. Durham, and E.W Rubel (1991) Afferent influences on brainstem auditory nuclei of the chicken: Neuron number and size following cochlea removal. Brain Res. *557:*37–47.

Brand, M.D. and M.P. Murphy (1987) Control of electron flux through the respiratory chain in mitochondria and cells. Biol. Rev. Camb. Phil. Soc. *62:*141–193.

Cheung, J.Y., J.V. Bonventre, C.D. Malis, and A. Leaf (1986) Calcium and ischemic injury. N. Engl. J. Med. *314:*1670–1676.

Choi, D.W. (1987) Ionic dependence of glutamate neurotoxicity in cortical cell culture. J. Neurosci. *7:*369–379.

Choi, D.W. (1988a) Glutamate neurotoxicity and diseases of the nervous system. Neuron *1:*623–634.

Choi, D.W. (1988b) Calcium-mediated neurotoxicity: Relationship to specific channel types and role in ischemic damage. TINS *11:*465–469

Clarke, P.G.H. (1990) Developmental cell death: morphological diversity and multiple mechanisms. Anat. Embryol. *181:*195–213.

Denton, R.M. and J.G. McCormack (1990) Ca^{2+} as a second messenger within mitochondria of the heart and other tissues. Annu. Rev. Physiol. *52:*451–466.

Durham, D. and E.W Rubel (1985) Afferent influences on brain stem auditory nuclei of the chicken: Changes in succinate dehydrogenase activity following cochlea removal. J. Comp. Neurol. *231:*446–456.

Durham, D., F.M. Matschinsky, and E.W Rubel (1993) Altered malate dehydrogenase activity in nucleus magnocellularis of the chicken following cochlea removal. Hear. Res. *70:*151–159.

Fein, A. and M. Tsacopoulos (1988) Activation of mitochondrial oxidative metabolism by calcium ions in *Limulus* ventral photoreceptor. Nature *331:*437–440.

Furber, S., R.W. Oppenheim, and D. Prevette (1987) Naturally-occurring neuron death in the ciliary ganglion of the chick embryo following removal of preganglionic input: Evidence for the role of afferents in ganglion cell survival. J. Neurosci. *7:*1816–1832.

Garden, G.A., K.S. Canady, D.I. Lurie, M. Bothwell, and E.W Rubel (1994) A biphasic change in ribosomal conformation during transneuronal degeneration is altered by inhibition of mitochondrial, but not cytoplasmic protein synthesis. J. Neurosci. *14:*1994–2008.

Garden, G.A., V. Redeker-DeWulf, and E.W Rubel (1995a) Changes in transcriptional activity of chicken auditory brainstem neurons following loss of afferent innervation. J. Comp. Neurol. *359:*412–423.

Garden, G.A., M. Hartlage-Rübsamen, E.W Rubel, and M. Bothwell (1995b) Protein masking of a ribosomal RNA epitope is an early event in afferent deprivation induced neuronal death. Molec. Cell. Neurosci. *6:*293–310.

Hallmann, M. (1973) Oxygen uptake in neonatal rats: a developmental study with particular reference to the effects of chloramphenicol. Paediatr. Res. *7:*923–930.

Herrington, J., B.P. Park, D.F. Babcock, and B. Hille (1996) Dominant role of mitochondria in clearance of large Ca^{2+} loads from rat adrenal chromatin cells. Neuron. *16:*119–228.

Hershey, J.W.B. (1990) Overview: Phosphorylation and translation control. Enzyme *44:*17–27.

Hockenbery, D.M., Z.N. Oltvai, X.M. Yin, C.L. Milliman, and S.J. Korsmeyer (1993) Bcl-2 functions in an antioxidant pathway to prevent apoptosis. Cell *75:*241–251.

Holt, D., D. Harvey, and R. Hurley (1993) Chloramphenicol toxicity. Adverse Drug React. Toxicol. Rev. *12:*83–95.

Hossmann, K.A. and P. Kleihues (1973) Reversibility of ischemic brain damage. Arch. Neurol. *29:*375–382.

Houge, G., S.O. Døskeland, R. Bøe, and M. Lanotte (1993) Selective cleavage of 28S rRNA variable regions V3 and V13 in myeloid leukemia cell apoptosis. FEBS Letters *315:*16–20.

Hyde, G.E. and D. Durham (1990) Cytochrome oxidase response to cochlea removal in chicken auditory brainstem neurons. J. Comp. Neurol. *297:*329–339.

Hyde, G.E. and D. Durham (1994a) Rapid increase in mitochondrial volume in nucleus magnocellularis neurons following cochlea removal. J. Comp. Neurol. *339:*27–48.

Hyde, G.E. and D. Durham (1994b) Increased deafferentation-induced cell death in chick brainstem auditory neurons following blockade of mito-

chondrial protein synthesis with chloramphenicol. J. Neurosci. *14:*291–300.

Jagus, R., W. French Anderson, and B. Safer (1981) The regulation of initiation of mammalian protein synthesis. In: Progress in Nucleic Acid Research and Molecular Biology, *25:*129–185. New York: Academic Press.

Jhaveri, S. and D.K. Morest (1982a) Neuronal architecture in nucleus magnocellularis of the chick auditory system with observations on nucleus laminaris: A light and electron microscope study. Neurosci. *7:*809–836.

Jhaveri, S. and D.K. Morest (1982b) Sequential alterations of neuronal architecture in nucleus magnocellularis of the developing chicken: An electron microscope study. Neurosci. *7:*855–870.

Jiménez, A. (1976) Inhibitors of translation. Trends Biochem. Sci. *1:*28–30.

Jones, D.A. and H. McIlwain (1971) Amino acid distribution and incorporation into proteins in isolated, electrically-stimulated cerebral tissues. J. Neurochem. *18:*41–58.

Kane, D.J., T.A. Sarafian, R. Anton, H. Hahn, E.B. Gralla, J.S. Valentine, T. Örd, and D.E. Bredesen (1993) Bcl-2 inhibition of neuronal cell death: Decreased generation of reactive oxygen species. Science *262:*1274–1277.

Kiessling, M., K. Weigel, D. Gartzen, and P. Kleihues (1982) Regional heterogeneity of L-[3-^{3}H] tyrosine incorporation into rat brain proteins during severe hypoglycemia. J. Cereb. Blood Flow Metab. *2:*249–253.

Kleihues, P. and K.A. Hossmann (1971) Protein synthesis in the cat brain after prolonged cerebral ischemia. Brain Res. *35:*409–418.

Krause, G.S. and B.R. Tiffany (1993) Suppression of protein synthesis in the reperfused brain. Stroke *24:*747–756.

Lamb, A.J., G.D. Clark-Walker, and A.W. Linnane (1968) The biogenesis of mitochondria: The differentiation of mitochondrial and cytoplasmic protein synthesizing systems *in vitro* by antibiotics. Biochem. Biophys. Acta *161:*415–427.

Lehninger, A.L. (1970) Mitochondria and Ca^{2+} ion transport. Biochem. J. *119:*129–138.

Lipton, P. (1987) Measurement of protein synthesis in hippocampal slices: *In vitro* versus *in vivo*. In A. Schurr, T.J. Teyler, and M.T. Tseng (eds): Brain Slices: Fundamentals, Applications and Implications. Switzerland: Karger.

Lipton, P., K. Raley, and D. Lobner (1988) Long-term inhibition of synaptic transmission and macromolecular synthesis following anoxia in the rat hippocampal slice: Interaction between Ca^{2+} and NMDA receptors. In G. Somjen (ed): Mechanisms of Cerebral Hypoxia and Stroke. New York: Plenum Press, pp. 229–249.

Mattson, M.P., Y. Zhang, and S. Bose (1993) Growth factors prevent mitochondrial dysfunction, loss of calcium homeostasis, and cell injury, but not ATP depletion in hippocampal neurons deprived of glucose. Exp. Neurol. *121:*1–13.

McConkey, D.J., P. Nicotera, P. Hartzell, G. Bellomo, A.H. Wyllie, and S. Orrenius (1989) Glucocorticoids activate a suicide process in thymocytes through an elevation of cytosolic Ca^{2+} concentration. Arch. Biochem. Biophys. *269:*365–370.

Merrick, W.C. (1990) Overview: Mechanism of translation initiation in eukaryotes. Enzyme *44:*7–16.

Montisano, D.F. and T.W. James (1979) Mitochondrial morphology in yeast with and without mitochondrial DNA. J. Ultrastruct. Res. *67:*288–296.

Moore, M.N. and L.L. Spremulli (1985) Effects of cations and cosolvents on eukaryotic ribosomal subunit conformation. Biochemistry *24:*191–196.

Morley, S.J. and G. Thomas (1991) Intracellular messengers and the control of protein synthesis. Pharmac. Ther. *50:*291–319.

Murray T., K.M. Dowey, and A.A. Yunis (1982) Degradation of isolated DNA mediated by nitroso-chloramphenicol: Possible role in chloramphenicol-induced aplastic anaemia. Biochem. Pharmacol. *31:*2291–2296.

O'Connor, T.M. and C.R. Wyttenbach (1974) Cell death in the embryonic chick spinal cord. J. Cell Biol. *60:*448–459.

Oppenheim, R.W. (1991) Cell death during development of the nervous system. Annu. Rev. Neurosci. 14:453–501.

Orrenius, S., D.J. McConkey, G. Bellomo, and P. Nicotera (1989) Role of Ca^{2+} in toxic cell killing. TiPS *10:*281–285.

Orrenius, S., M.J. McCabe, and P. Nicotera (1992) Ca^{2+}— dependent mechanisms of cytotoxicity and programmed cell death. Toxicol. Lett. *64/65:*357–364.

Panniers, R. and E. Henshaw (1983) A GDP/GTP exchange factor essential for recycling in Erlich ascites tumor cells and its regulation by eukaryotic initiation factor 2 phosphorylation. J. Biol. Chem. *258:*7928–7934.

Parks, T.N. (1981) Morphology of axosomatic endings in an avian cochlear nucleus: Nucleus magnocellularis of the chicken. J. Comp. Neurol. *203:*425–440.

Pilar, G. and L. Landmesser (1976) Ultrastructural differences during embryonic death in normal and peripherally deprived ciliary ganglia. J. Cell Biol. *68:*339–356.

Prentki, M., C.B. Wollheim, and P.D. Lew (1984) Ca^{2+} homeostasis in permeabilized human neutrophils: Characterization of Ca^{2+} sequestering pools and the action of inositol 1,4,5-triphosphate. J. Biol. Chem. *259:*13777–13782.

Raley-Susman, K.M. and P. Lipton (1990) In vitro ischemia and protein synthesis in the rat hippocampal slice: The role of calcium and NMDA receptor activation. Brain Res. *515:*27–38.

Randall, R.D. and S.A. Thayer (1992) Glutamate-induced calcium transient triggers delayed Calcium overload and neurotoxicity in rat hippocampal neurons. J. Neurosci. *12:*1882–1895.

Rhoads, R.E. (1993) Regulation of eukaryotic protein synthesis by initiation factors. J. Biol. Chem. *268:*3017–3020.

Richter, C. and G.E.N. Kass (1991) Oxidative stress in mitochondria: Its relationship to cellular Ca^{2+} homeostasis, cell death, proliferation, and differentiation. Chem. Biol. Interactions *77:*1–23.

Rubel, E.W, R.L. Hyson, and D. Durham (1990) Afferent regulation of neurons in the brain stem auditory system. J. Neurobiol. *21:*169–196.

Rubel, E.W, P.M. Falk, K.S. Canady, and O. Steward (1991) A cellular mechanism underlying activity-dependent transneuronal degeneration: Rapid but reversible destruction of neuronal ribosomes. Brain Dysfunct. *4:*55–74.

Sarre, T.F. (1989) The phosphorylation of eukaryotic initiation factor 2: A principle of translational control in mammalian cells. Biosystems *22:*311–325.

Siesjö, B.K. (1988) Calcium, ischemia and death of brain cells. Ann. NY Acad. Sci. *522:*638–661.

Simon, R.P., T. Griffith, M.C. Evans, J.H. Swan, and B.S. Meldrum (1984) Calcium overload in selectively vulnerable neurons of the hippocampus during and after ischemia: An electron microscope study in the rat. J. Cereb. Blood Flow Metabol. *4:*350–361.

Steitz, J.A. (1989) Immunoprecipitation of ribonucleoproteins using autoantibodies. Methods in Enzymol. *180:*468–481.

Steward, O. and E.W Rubel (1985) Afferent influences on brain stem auditory nuclei of the chicken: Cessation of amino acid incorporation as an antecedent to age-dependent transneuronal degeneration. J. Comp. Neurol. *231:*385–395.

Tocher, J.H., R.C. Knight, and D.I. Edwards (1988) Electrochemical characteristics of nitro-heterocyclic compounds of biological interest: II. Nitroso-chloramphenicol. Free Radical Res. Commun. *5:*319–326.

Trump, B.F. and I.K. Berezesky (1992) The role of cytosolic Ca^{2+} in cell injury, necrosis and apoptosis. Curr. Opinion Cell Biol. *4:*227–232.

Tzagoloff, A. (1982) Mitochondria. New York:Plenum.

Tzagoloff, A. and A.M. Myers (1986) Genetics of mitochondrial biogenesis. Ann Rev Biochem. *55:*249–285.

Vornov, J.J. and J.T. Coyle (1991) Glutamate neurotoxicity and the inhibition of protein synthesis in the hippocampal slice. J. Neurochem. *56:*996–1006.

Werth, J.L. and S.A. Thayer (1994) Mitochondria buffer physiological calcium loads in cultured rat dorsal root ganglion neurons. J. Neurosci. *14:*348–356.

Widman, R., T. Kuroiwa, P. Bonnekoh, and K.A. Hossmann (1991) [^{14}C]Leucine incorporation into brain proteins in gerbils after transient ischemia: Relationship to selective vulnerability of hippocampus. J. Neurochem. *56:*789–796.

Yunis, A.A. (1988) Chloramphenicol: Relation of structure to activity and toxicity. Annu. Rev. Pharmacol. Toxicol. *28:*83–100.

Zirpel, L., E.A. Lachica, and W.R. Lippe (1995) Deafferentation increases the intracellular calcium of cochlear nucleus neurons in the embryonic chick. J. Neurophysiol. *74:*1355–1357.

Zirpel, L. and E.W Rubel (1996) Eighth nerve activity regulates intracellular calcium concentration of avian cochlear nucleus neurons via a metabotropic glutamate receptor. J. Neurophysiol. (in press).